

A preliminary model study of the equine back including activity of *longissimus dorsi* muscle

M. GROESEL^{*†}, R. R. ZSOLDOS, A. KOTSCHWAR, M. GFOEHLER[†] and C. PEHAM

Movement Science Group Vienna, Clinic of Orthopaedics in Ungulates, University of Veterinary Medicine Vienna, Vienna, Austria; and

[†]Institute for Engineering Design and Logistic Engineering, Machine Design and Rehabilitation Engineering, Vienna University of Technology, Vienna, Austria.

Keywords: horse; back movement; biomechanical model; *longissimus dorsi*; lateral bending

Summary

Reasons for performing study: Identifying the underlying problem of equine back pain and diseases of the spine are significant problems in veterinary orthopaedics. A study to validate a preliminary biomechanical model of the equine back based on CT images including *longissimus dorsi* (LD) muscle is therefore important.

Objectives: Validation of the back model by comparing the shortening of LD muscles in the model with integrated EMG (IEMG) at stance during induced lateral flexion of the spine.

Methods: *Longissimus dorsi* muscle activity at stance has been used for validation. EMG electrodes were placed laterally at the level of T12, T16 and L3. Reflective markers have been attached on top of the spinous processes T5, T12, T16, L1 and the sacral bone (OS1, OS2) for motion tracking analysis. A virtual model of the equine's back (T1–S5) was built with inclusion of a simplified LD muscle by 2 separate contours left and right of the spine, starting at *tuber coxae* laterally and attaching to the spinous process T5 medially. Shortening of LD during induced lateral flexion caused by the kinematic data (input) was compared to the 3 EMG signals (T12, T16 and L3) on the active side via correlation.

Results: Pearson correlation coefficient between IEMG and shortening length of LD in the model was (mean \pm s.d.) 0.95 ± 0.07 for the left side and 0.91 ± 0.07 for the right side of LD.

Conclusions: Activity of the LD muscles is mainly responsible for stabilisation of the vertebral column with isometric muscle contraction against dynamic forces in walk and trot. This validation requires muscle shortening in the back, like induced lateral flexion at stance. The length of the shortening muscle model and the IEMG show a linear relationship. These findings will help to model the LD for forward simulations, e.g. from force to motion.

Introduction

Back pain and diseases of the vertebral column and spinal cord have become recognised as an important cause of reduced performance in horses over the past few decades (Jeffcott 1995). It is well known that diagnosis of back problems is difficult and the

application of sophisticated clinical aids (e.g. radiology, ultrasonography and scintigraphy) is not satisfying in most cases. Definitive diagnosis of back injury is often made by elimination of all other possible causes.

The functional anatomy and the kinematics of the thoracolumbar spine have been studied widely in the past (Townsend *et al.* 1983; Pourcelot *et al.* 1998; Audigié *et al.* 1999; Denoix 1999). The largest muscle in the equine back is the *longissimus dorsi* which originates at the spinous processes of the sacrum, lumbar and thoracic vertebrae and wing of the ilium and the insertions are to the transverse processes and tubercles of the ribs (Budras *et al.* 2003). This epaxial muscle plays an important role in locomotion ability and performance in the horse. It can both provide stiffness to the joints and provide the bending moments required for enabling joint motion (Rituechai *et al.* 2008). Its anatomical position makes it possible to produce extension, lateral flexion and axial rotation moments about the spine (Haussler 1999). In previous studies the EMG activity of the *longissimus dorsi* muscle has been studied during walk and trot on a treadmill and with induced back movements at stance (Peham *et al.* 2001; Robert *et al.* 2001a,b; Licka *et al.* 2004, 2009).

The aim of this study was to perform a first validation of a preliminary biomechanical model of the thoracic and lumbar spine combined with the activity of the *longissimus dorsi* muscle. The validation was done during induced lateral bending at stance by comparing the muscle shortening with the IEMG of *longissimus dorsi* muscle.

Materials and methods

Experimental data

Three-dimensional kinematic data were collected from 10 horses (age 5–20 years, weight 450–700 kg, of various breeds) without clinical signs of back pain.

Measurements were performed using 10 cameras for kinematic motion analysis (Eagle Digital, sample frequency 120 Hz)¹ together with a simultaneously triggered EMG telemetric system (Telemyo Mini 16, sample frequency 1.2 kHz)². After palpation reflective markers were placed on the dorsal spinous processes of T5, T12, T16, L1 and on the sacral bone (*os sacrum*, OS1, OS2).

*Corresponding author email: martin.groesel@vetmeduni.ac.at

[Paper received for publication 08.01.10; Accepted 26.06.10]

The placement of surface EMG electrodes was similar to that described by Peham *et al.* (2001), situated bilaterally on the shaved skin above *longissimus dorsi* muscle at the level of spinous process of T12, T16 and L3. The distance between the bipolar electrodes was about 4 cm, according to EMG guidelines (Soderberg 1992). Measurements were obtained during a period of 5 s, 3 trials on both sides. Pushing a blunt object into the *M. longissimus* between T12 and T16 induced lateroflexion. The back movements were provoked by the same examiner in all horses. Experimental data were post processed by Cortex 1.1 software¹.

Material and method for the biomechanical model

The spine of a 13-year-old Irish Thoroughbred mare (550 kg) was obtained from *post mortem* material. The back was prepared by trimming the rib cages to be less than 0.45 m in width; axial CT scans of the back from T1–S5 were performed by a spiral CT scanner (GE HiSpeed DX/i)³ and 505 slices were acquired corresponding to a 3 mm reconstructed slice thickness. Each slice consisted of a 512 x 512 array with a pixel size of 0.98 mm, with x-ray tube voltage of 120 kV and x-ray tube current of 60 mA.

The virtual biomodel based on CT scans was built with 2D and 3D CAD software according to Groesel *et al.* (2009).

Back model

The first step was to build a model of the equine spine in the musculoskeletal modelling environment SIMM⁴ (Delp *et al.* 1990; Delp and Loan 1995), which is a simulation software that enables users to create, alter and evaluate models of many different musculoskeletal structures (Vasavada *et al.* 1998; Holzbaur *et al.* 2005; Hutchinson *et al.* 2005). Designed in the early 1990s, SIMM is now used by hundreds of biomechanics researchers to create computer models of musculoskeletal structures and to simulate movements (Delp *et al.* 2007). SIMM has helped bring simulations to biologists who have created computational models of the frog (Kargo and Rome 2002; Kargo *et al.* 2002), cockroach (Full and Ahn 1995), *Tyrannosaurus rex* (Hutchinson *et al.* 2005) and other animals.

The virtual spine consisted of 26 segments (*os sacrum* and hip bone, 6 lumbar and 18 thoracic vertebrae) and 24 joints. Movement between *os sacrum* and the hip bone was blocked. In this opening study the degrees of freedom (DOF) were limited to lateral bending (LB) (Fig 1). For the first testing methods the maximum range of motion (ROM) was taken from cadaveric studies published by Townsend *et al.* (1983). Maximum ROM for lateral bending was defined as $\pm 3^\circ$ in each joint. The model of *M. longissimus dorsi* was a combination of the different regions of the muscle explained by Ritruethchai *et al.* (2008) with its mediolateral and dorsoventral fascicle orientations. As an initial approximation the simplified *longissimus dorsi* muscle had its origin at *tuber coxae* and insertion in the lower lateral part of the spinous process of T5 (Fig 2). The first marker on the thoracic spine was placed on T5. Caudally of T5 no kinematic data were available and therefore a continuation of LD was not necessarily required. The model of LD was a compromise between fibre orientation and origin and insertion of its aponeurosis; especially for its role as a stabiliser of the vertebral column.

In the second step, the SIMM model was exported to OpenSim; an open-source software for modelling, simulating and analysing musculoskeletal models (Delp *et al.* 2007). The back model was

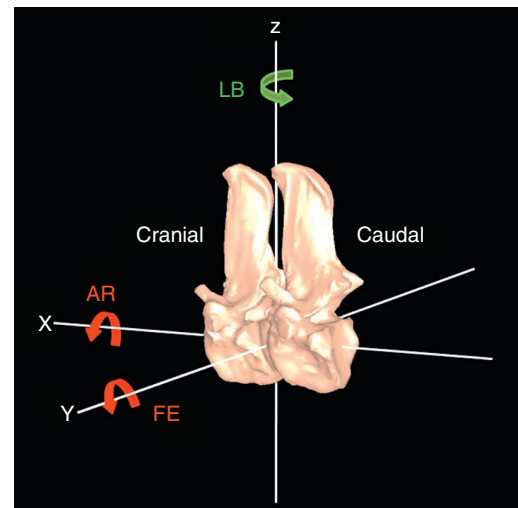


Fig 1: Lateral view of the degrees of freedom shown by joint axes between T15 and T16. A standard right-handed orthogonal Cartesian coordinate system was used to describe spinal rotations. In the laboratory coordinate system the x axis was aligned with the line of progression, being positive cranially. The z axis was defined as perpendicular to the x axis, vertically and being positive upwards. The positive y axis was perpendicular to these 2 axes, to the left. Consequently, axial rotation (AR) was defined as a rotation around the x axis, flexion-extension (FE) a rotation around y axis and lateral bending (LB) rotation around the z axis.

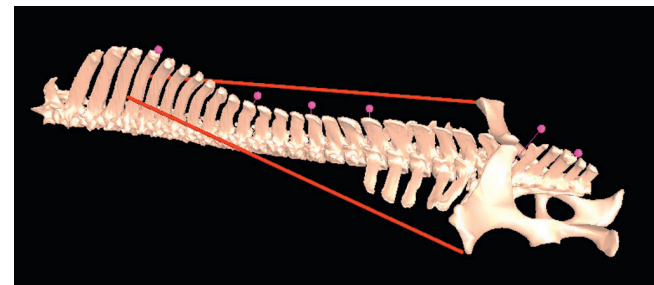


Fig 2: Model of the equine thoracolumbar spine built in SIMM starting with the first thoracic vertebra on the left alternating back to *os sacrum* and the hip bone on the right. Six markers were defined on top of spinous processes of T5, T12, T16, L1 and 2 at the sacral bones. In this preliminary model *longissimus dorsi* muscle had its origin at the *tuber coxae* on the hip bone and its insertion to the fifth thoracic vertebra. The model of LD is a compromise solution between fibre orientation and origin and insertion of its aponeurosis.

scaled to match the anthropometry of the actually measured horse, based on the marker positions. Muscle length was also scaled automatically so that *longissimus dorsi* muscle remained the same percentage of the original model.

In the third step, the inverse kinematics (IK) were resolved to determine the model generalised coordinate values (joint angles and translations), based on motion tracking data.

The changes in distance between the experimental markers and corresponding markers on the scaled model were calculated using a 3D root mean square error analysis method (Table 2).

Analysis methods

The EMG signal was rectified and the sampling rate reduced to 120 Hz to make EMG and motion data comparable. This undersampling technique was achieved by calculating the mean of

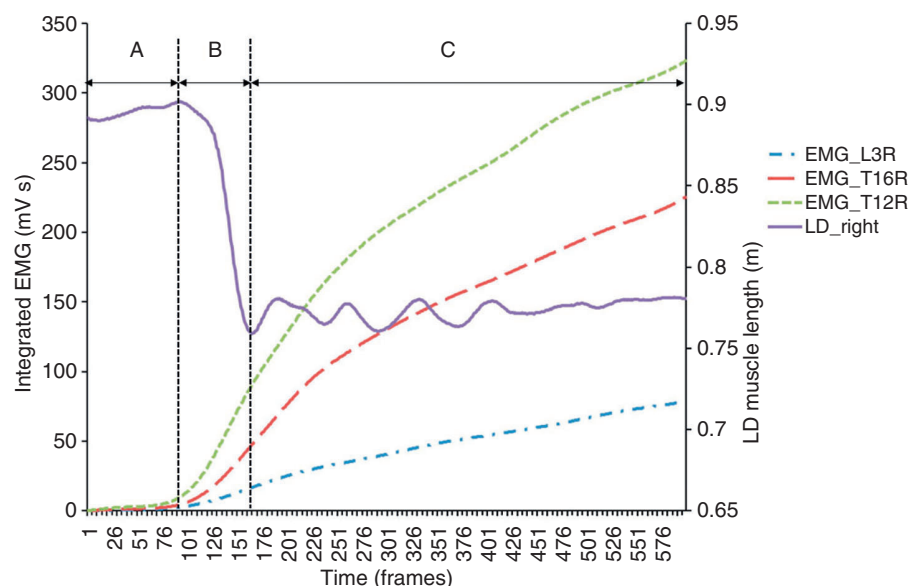


Fig 3: Comparison of integrated EMG with shortening muscle length data calculated in OpenSim. Part A shows the initial relaxed position without muscle activity or mentionable movement. Section B was the part of interest, where the model's length of longissimus dorsi muscle was changing due to lateroflexion calculated from kinematic data. Part C shows a more or less constant muscle length, but as a result of isometric muscle contraction a strong EMG signal was still recorded. For that reason, section C was not qualified for correlation.

TABLE 1: Correlation of all 10 horses with 30 induced lateral bending measurements including 3 EMG electrodes per side

	Position EMG signal					
	Left			Right		
	L3	T16	T12	L3	T16	T12
Correlation	0.95	0.95	0.95	0.92	0.92	0.91
s.d.	0.04	0.04	0.03	0.07	0.07	0.07
Range	0.87–0.99	0.86–0.99	0.89–0.99	0.75–0.99	0.76–0.66	0.74–0.99

The table shows the correlation coefficients of the active shortening muscles with the local surface IEMG signals.

10 samples. The final step in the calculation was the application of a Butterworth low pass filter, 7th order and cut-off frequency of 10 Hz. This filter technique was successfully used in previous studies from Peham *et al.* (2001) and Licka *et al.* (2009). The smoothed EMG data were integrated in order to be comparable with the shortening of *M. longissimus dorsi*. Pearson correlations coefficients were calculated from the beginnings of lateroflexion to maximum bending (Fig 3). Three trials to the left and 3 to the right were measured (60 trials). From each trial the shortening of the muscle in the model was correlated with each of the 3 IEMG signals (T12, T16, L3) of the active side. The correlation coefficients were grouped and mean \pm s.d. determined. Therefore, the motion sequence (Fig 3) was divided into 3 sections. The first part (A) was the relaxed position of *longissimus dorsi* muscle before lateral bending reflex was induced. In section B, EMG data and lateral flexion of the model were correlated. In part C, where lateral movement of the back already came to an end, continued strong EMG signal was recorded as a result of isometric muscle contraction. This section was, like the first part, not appropriate for correlation.

Results

During induced lateral bending to the left, correlation coefficients (mean \pm s.d.) between IEMG and concentric shortening muscle

model were 0.95 ± 0.04 at level L3, 0.95 ± 0.04 at T16 and 0.95 ± 0.03 at T12. For the right part the mean correlation coefficients were lower, with 0.92 ± 0.07 at L3 and T16 and 0.91 ± 0.07 at level T12 (Table 1). There was no significant difference between the 6 EMG positions ($P > 0.05$).

Mean ROM in the joints of the model were $2.02^\circ \pm 0.37$ for bending the middle of the back to the right and $2.11^\circ \pm 0.65$ to the left. Maximum movement was 2.63° to the right and 2.86° to the left in each joint.

Figure 4 shows an example of the linear relationship between the integrated EMG and the length of shortening muscle.

The mean values of marker error calculated in OpenSim for all 10 horses are listed in Table 2. The changes in distance between the experimental marker and the corresponding marker on the model are shown in Figure 5 on one specific lateral bending measurement. The maximum biases between markers were located on T5 with 4.6 mm and on T12 with 5.4 mm in different horses.

Discussion

During the described induced reflex on a horse's back, LD muscles were mainly active and responsible for lateral bending (Licka and Peham 1998; Peham *et al.* 2001). It was assumed that there is a linear relationship between the IEMG of LD and the

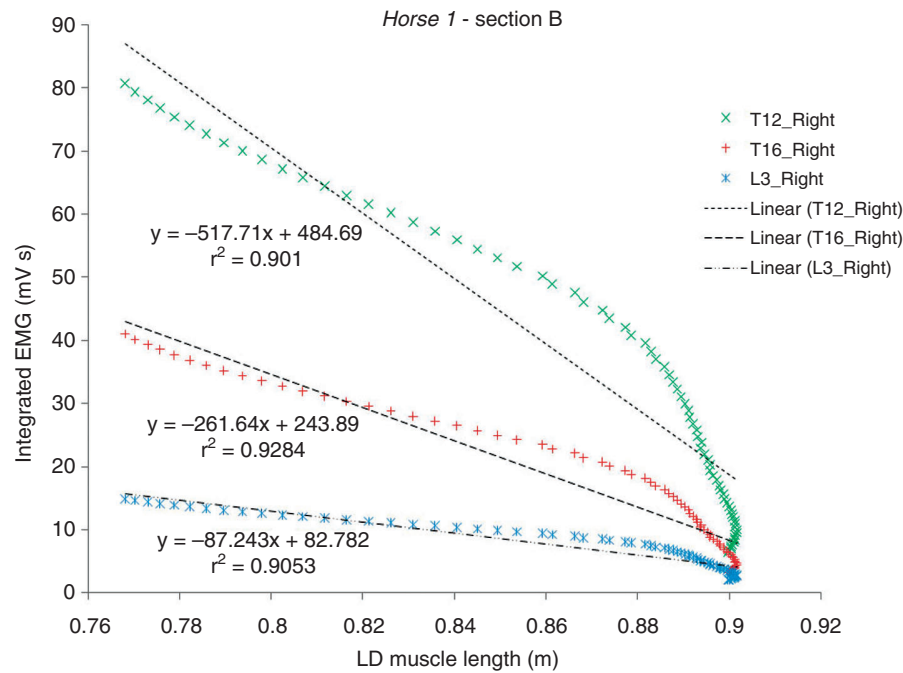


Fig 4: Linear relationship of the third trial on Horse 1 between the integrated EMG and the length of shortening LD muscle in section B as explained in Figure 3.

TABLE 2: Mean \pm s.d. values in millimetres of the range of marker errors of the 6 skin markers calculated in OpenSim for all 10 horses

Marker error in (mm)		Horse									
		1	2	3	4	5	6	7	8	9	10
T5	Mean	1.5	1.0	0.9	1.0	1.0	0.9	1.2	1.0	1.6	1.4
	s.d.	0.4	0.2	0.3	0.2	0.3	0.2	0.3	0.2	1.0	0.5
T12	Mean	0.9	0.6	0.6	0.6	0.7	0.6	0.9	0.7	0.9	1.3
	s.d.	0.3	0.3	0.2	0.1	0.3	0.2	0.4	0.2	0.4	0.7
T16	Mean	0.8	0.5	0.5	0.4	0.5	0.4	0.6	0.4	0.7	0.8
	s.d.	0.3	0.2	0.1	0.3	0.2	0.2	0.2	0.2	0.3	0.4
L1	Mean	0.8	0.4	0.4	0.4	0.5	0.4	0.6	0.4	0.7	0.8
	s.d.	0.3	0.1	0.2	0.3	0.2	0.1	0.2	0.2	0.4	0.4
OS1	Mean	0.7	0.5	0.4	0.4	0.6	0.5	0.6	0.6	0.9	0.9
	s.d.	0.2	0.1	0.1	0.2	0.4	0.2	0.2	0.3	0.4	0.2
OS2	Mean	0.8	0.5	0.4	0.3	0.6	0.5	0.6	0.6	1.0	1.0
	s.d.	0.3	0.1	0.2	0.2	0.3	0.3	0.3	0.2	0.5	0.2

A marker error is the distance between the experimental marker and the corresponding marker on the scaled back model.

shortening length of the muscle in the model (Guimaraes *et al.* 1994a,b, 1995).

Correlation for the right part of the back is in general about 3% lower than for the left side. One reason could be the different position of the segment and joint axes in the bones. As shown in Figure 1, the axes should be centred in the exact middle of the body of the vertebrae. During model development in SIMM, all axes had to be placed manually and this can cause marginal variation of the axes of rotation and influence their final movement in the model (Arnold *et al.* 2000). The segment's centre of rotation has high influences in the resulting moment arms and accuracy of a biomechanical model (Delp *et al.* 1994; Pandy 1999). However, we are convinced that the potential error in joint axes estimation is presumably small enough to avoid changing our conclusions. It can be assumed that the difference of 3% in the correlation coefficients between left and right is affected by the low amount of measured horses.

Influences such as skin thickness, distribution of sweat glands, sweating and subcutaneous fat can also lead to a large variation in magnitude of surface EMG recordings (Nordander *et al.* 2003). Another reason could be undetected presence of back pain in some horses, which can lead to activation imbalances and neuromuscular fatigue in spine muscles (Oddsson and De Luca 2003). Different maximum muscle activity values for left and right side on equine back muscles are also published by Zaneb *et al.* (2009) and the preferential use of muscles on one side over the other as a consequence of the 'handedness' of the horses should be considered (Whelan 2003). This may be the cause for the differences found between left and right measurements.

This study was a preliminary validation of the current model with only 6 markers. To be able to calculate the exact position of each bone at all time, a minimum of 3 markers per segment is recommended. Placing more than 3 markers per segment would even give the possibility to reduce the digitisation errors by least

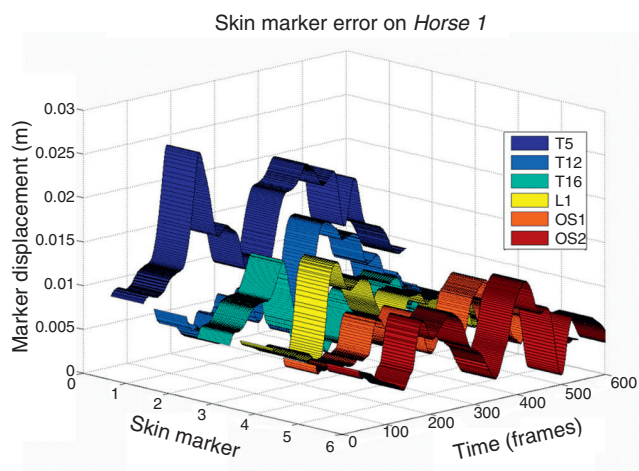


Fig 5: Differences between skin marker positions in the model and the experimental markers on the horse as a range of error. A summary of all marker error values is shown in Table 2.

squares averaging techniques. Future measurements will include additional skin markers, nevertheless they always cause small-sized systematic errors in calculation of movements, forces and torques as a consequence of the movement of the skin with respect to the underlying bone (Kingma *et al.* 1996; Leardini *et al.* 2005). The marker movements could be corrected based on algorithms developed from studies using bone-fixed markers (van Weeren and Barneveld 1986; Faber *et al.* 2000, 2001; Khumsap *et al.* 2004; Sha *et al.* 2004), but such investigations are highly invasive, require local anaesthesia and bone-pins sticking through skin and muscles may influence the physiological movement. In our study, the effect of marker displacement due to skin movement was not further investigated, but it can be expected to be small as the back of horses has a tight skin covering and overall mobility is low (Clancy *et al.* 2002).

The hip bone, as the biggest segment in the model, should have 3 or even 4 skin markers, for example 2 on spinous processes of *os sacrum* and left and right at *tuber coxae*. To place 3 skin markers per vertebra is hard to realise on a horse's back and the kinematic data is always likely to be defective due to skin movement (Licka *et al.* 2001a,b).

Blocked axial rotation (AR) and flexion-extension (FE) should decrease the DOF to a minimum required for this preliminary validation. A model with 26 segments and only 6 markers is a mathematically underdetermined system. The number of unknowns should be decreased and/or the number of system equations increased until the number of unknowns and system equations match (Morrison 1968; Pierrynowski and Morrison 1985). Therefore, the 24 joints had the same ROM, defined by one single function. Otherwise, inverse kinematic calculation would result in an unlimited number of possible solutions.

EMG data from surface electrode at level T12 is in general additionally affected by *M. latissimus dorsi* and *M. rhomboideus thoracis* by myoelectric signal crosstalk (DeLuca and Merletti 1988; Winter *et al.* 1994). Due to the fact that the lateral bending was an initiated reflex at stance, only *M. longissimus dorsi* was mainly active.

In the study by Tokuriki *et al.* (1997), the LD of the horse seems to play a role in limiting lateral bending of the trunk during walk and trot. During the suspension phase at trot, it acts to stabilise the thoracolumbar spine undergoing passive flexion (Denoix and

Audigié 2001). The chosen method is simple and perhaps the only possibility to compare the muscle shortening in the model with IEMG data.

The simplification of the model limited the results, so further developments are necessary to make a step closer to reality. Suggestions for improvements are an extended marker set to allow more DOF and a higher complexity of the model.

Future studies will also include a more precise definition of *longissimus dorsi* muscles (Wakeling *et al.* 2007; Ritruethai *et al.* 2008). In the presented model the geometry of muscle actuators is defined by 2 points, which are connected by line segments. This is reasonable for muscles with small areas of origin and insertion. For LD with large areas of attachment and multiple origins of the aponeurosis and the muscle fibres, a volumetric object would be a more realistic model. As a compromise, muscles with multiple or large attachment areas can be split into any number of compartments (Delp and Loan 1995). Every single part of the muscle will then span one joint and will develop force, thus generating moments about this joint.

The segments in future models should also include mass, mass centre and moment of inertia for inverse dynamic (ID) simulations (Buchner *et al.* 1997).

To achieve an even more realistic model, the continuity with the neck would be an important extension. If these steps are realised, the result will be forces, torques and loads acting in the thoracolumbar joints and identifying peak concentrations, allowing new insights into the different pathogeneses of chronic back pain.

Acknowledgements

This modelling study was realised in the framework of the project 'Biomechanical, anatomy-based model of the equine spine' (P19506-N14), sponsored by the Austrian Science Fund (FWF).

Conflicts of interest

The authors declare no potential conflicts.

Manufacturers' addresses

¹Motion Analysis Corp., Santa Rosa, California, USA.

²Noraxon Inc., Scottsdale, Arizona, USA.

³General Electric Company, Fairfield, Connecticut, USA.

⁴MusculoGraphics Inc., Santa Rosa, California, USA.

References

- Arnold, A.S., Salinas, S., Asakawa, D.J. and Delp, S.L. (2000) Accuracy of muscle moment arms estimated from MRI-based musculoskeletal models of the lower extremity. *Comput. Aided Surg.* **5**, 108-119.
- Audigié, F., Pourcelot, P., Degueurce, C., Denoix, J.M. and Geiger, D. (1999) Kinematics of the equine back: flexion-extension movements in sound trotting horses. *Equine vet. J., Suppl.* **30**, 210-213.
- Buchner, H.H.F., Savelberg, H.H.C.M., Schamhardt, H. and Barneveld, A. (1997) Inertial properties of dutch warmblood horses. *J. Biomech.* **30**, 653-658.
- Budras, K.D., Sack, W.O. and Röck, S. (2003) *Anatomy of the Horse: An Illustrated Text*, Schlütersche, Hannover. p 89.
- Clancy, E.A., Morin, E.L. and Merletti, R. (2002) Sampling, noise-reduction and amplitude estimation issues in surface electromyography. *J. Electromyogr. Kinesiol.* **12**, 1-16.
- Delp, S.L., Loan, J.P., Hoy, M.G., Zajac, F.E., Topp, E.L. and Rosen, J.M. (1990) An interactive graphics-based model of the lower extremity to study orthopaedic surgical procedures. *IEEE Trans. Biomed. Eng.* **37**, 757-767.

- Delp, S.L., Ringwelski, D.A. and Carroll, N.C. (1994) Transfer of the rectus femoris: effects of transfer site on moment arms about the knee and hip. *J. Biomech.* **27**, 1201-1211.
- Delp, S.L. and Loan, J.P. (1995) A graphics-based software system to develop and analyze models of musculoskeletal structures. *Comput. Biol. Med.* **25**, 21-34.
- Delp, S.L., Anderson, F.C., Allison, A., Loan, P., Habib, A., John, C., Guendelmann, E. and Thelen, D. (2007) OpenSim: open-source software to create and analyze dynamic simulations of movement. *IEEE Trans. Biomed. Eng.* **54**, 1940-1950.
- DeLuca, C.J. and Merletti, R. (1988) Surface myoelectric signal cross-talk among muscles of the leg. *Electroencephalogr. Clin. Neurophysiol.* **69**, 568-575.
- Denoix, J.M. (1999) Spinal biomechanics and functional anatomy. *Vet. Clin. N. Am.: Equine Pract.* **15**, 27-60.
- Denoix, J.M. and Audigié, F. (2001) *The Neck and Back*, W.B. Saunders Co., London.
- Faber, M., Schamhardt, H., van Weeren, P.R., Johnston, C., Roepstorff, L. and Barneveld, A. (2000) Basic three-dimensional kinematics of the vertebral column of horses walking on a treadmill. *Am. J. vet. Res.* **61**, 399-406.
- Faber, M., Johnston, C., Schamhardt, H., van Weeren, P.R., Roepstorff, L. and Barneveld, A. (2001) Basic three-dimensional kinematics of the vertebral column of horses trotting on a treadmill. *Am. J. vet. Res.* **62**, 757-764.
- Full, R.J. and Ahn, A.N. (1995) Static forces and moments generated in the insect leg: Comparison of a three-dimensional musculo-skeletal computer model with experimental measurements. *J. expt. Biol.* **198**, 1285-1298.
- Groessel, M., Gfoehler, M. and Peham, C. (2009) Alternative solution of virtual biomodeling based on CT-scans. *J. Biomech.* **42**, 2006-2009.
- Guimaraes, A.C., Herzog, W., Allinger, T.L. and Zhang, Y.T. (1995) The EMG-force relationship of the cat soleus muscle and its association with contractile conditions during locomotion. *J. expt. Biol.* **198**, 975-987.
- Guimaraes, A.C., Herzog, W., Hulliger, M., Zhang, Y.T. and Day, S. (1994a) Effects of muscle length on the EMG-Force relationship of the cat soleus muscle studied using non-periodic stimulation of ventral root filaments. *J. expt. Biol.* **193**, 49-64.
- Guimaraes, A.C., Herzog, W., Hulliger, M., Zhang, Y.T. and Day, S. (1994b) EMG-force relationship of the cat soleus muscle studied with distributed and non-periodic stimulation of ventral root filaments. *J. expt. Biol.* **186**, 75-93.
- Haussler, K.K. (1999) Anatomy of the thoracolumbar vertebral region. *Vet. Clin. N. Am.: Equine Pract.* **15**, 13-26.
- Holzbaur, K.R., Murray, W.M. and Delp, S.L. (2005) A model of the upper extremity for simulating musculoskeletal surgery and analyzing neuromuscular control. *Ann. Biomed. Eng.* **33**, 829-840.
- Hutchinson, J.R., Anderson, F.C., Blemker, S.S. and Delp, S.L. (2005) Analysis of hindlimb muscle moment arms in *Tyrannosaurus rex* using a three-dimensional musculoskeletal computer model: Implications for stance, gait, and speed. *Paleobiology* **31**, 676-701.
- Jeffcott, L.B. (1995) *The Approach to the Back of the Horse*, P.F.Knezevic (Hrsg.), Stuttgart. pp 316-326.
- Kargo, W.J. and Rome, L.C. (2002) Functional morphology of proximal hindlimb muscles in the frog *Rana pipiens*. *J. expt. Biol.* **205**, 1987-2004.
- Kargo, W.J., Nelson, F. and Rome, L.C. (2002) Jumping in frogs: Assessing the design of the skeletal system by anatomically realistic modeling and forward dynamic simulation. *J. expt. Biol.* **205**, 1683-1702.
- Khumsap, S., Lanovaz, J.L. and Clayton, H.M. (2004) Verification of skin-based markers for 3-dimensional kinematic analysis of the equine tarsal joint. *Equine vet. J.* **36**, 655-658.
- Kingma, I., de Looze, M.P., Toussaint, H.M., Klijnsma, H.G. and Bruijnen, T.B.M. (1996) Validation of a full body 3-D dynamic linked segment model. *Hum. Mov. Sci.* **15**, 833-860.
- Leardini, A., Chiari, L., Della Croce, U. and Cappozzo, A. (2005) Human movement analysis using stereophotogrammetry Part 3. Soft tissue artifact assessment and compensation. *Gait Posture* **21**, 212-225.
- Licka, T. and Peham, C. (1998) An objective method for evaluating the flexibility of the back of standing horses. *Equine vet. J.* **30**, 412-415.
- Licka, T., Peham, C. and Zohmann, E. (2001a) Range of back movement at trot in horses without back pain. *Equine vet. J., Suppl.* **33**, 150-153.
- Licka, T., Peham, C. and Zohmann, E. (2001b) Treadmill study of the range of back movement at the walk in horses without back pain. *Am. J. vet. Res.* **62**, 1173-1179.
- Licka, T., Peham, C. and Frey, A. (2004) Electromyographic activity of the longissimus dorsi muscles in horses during trotting on a treadmill. *Am. J. vet. Res.* **65**, 155-158.
- Licka, T., Frey, A. and Peham, C. (2009) Electromyographic activity of the longissimus dorsi muscles in horses when walking on a treadmill. *Vet. J.* **180**, 71-76.
- Morrison, J.B. (1968) Bioengineering analysis of force actions transmitted by the knee joint. *Biomed. Eng.* **3**, 164-170.
- Nordander, C., Willner, J., Hansson, G.A., Larsson, B., Unge, J., Granquist, L. and Skerfving, S. (2003) Influence of the subcutaneous fat layer, as measured by ultrasound, skinfold calipers and BMI, on the EMG amplitude. *Eur. J. appl. Physiol.* **89**, 514-519.
- Oddsson, L.I. and De Luca, C.J. (2003) Activation imbalances in lumbar spine muscles in the presence of chronic low back pain. *J. appl. Physiol.* **94**, 1410-1420.
- Pandy, M.G. (1999) Moment arm of a muscle force. *Exerc. Sport Sci. Rev.* **27**, 79-118.
- Peham, C., Frey, A., Licka, T. and Scheidl, M. (2001) Evaluation of the EMG activity of the long back muscle during induced back movements at stance. *Equine vet. J., Suppl.* **33**, 165-168.
- Pierrynowski, M.R. and Morrison, J.B. (1985) Estimating the muscle forces generated in the human lower extremity when walking: a physiological solution. *Math. Biosci.* **75**, 43-68.
- Pourcelot, P., Audigié, F., Degueurce, C., Denoix, J.M. and Geiger, D. (1998) Kinematics of the equine back: a method to study the thoracolumbar flexion-extension movements at the trot. *Vet. Res.* **29**, 519-525.
- Ritruethai, P., Weller, R. and Wakeling, J.M. (2008) Regionalisation of the muscle fascicle architecture in the equine longissimus dorsi muscle. *Equine vet. J.* **40**, 246-251.
- Robert, C., Audigié, F., Valette, J.P., Pourcelot, P. and Denoix, J.M. (2001a) Effects of treadmill speed on the mechanics of the back in the trotting saddlehorse. *Equine vet. J., Suppl.* **33**, 154-159.
- Robert, C., Valette, J.P. and Denoix, J.M. (2001b) The effects of treadmill inclination and speed on the activity of three trunk muscles in the trotting horse. *Equine vet. J.* **33**, 466-472.
- Sha, D.H., Mullineaux, D.R. and Clayton, H.M. (2004) Threedimensional analysis of patterns of skin displacement over the equine radius. *Equine vet. J.* **36**, 665-670.
- Soderberg, G.L. (1992) Recording techniques. In: *Selected Topics in Surface Electromyography for Use in Occupational Settings: Experts Perspectives*, Ed: Gary L. Soderberg, US Department of Health and Human Services Public Health Service, Center of Disease Control, National Institute for occupational Safety and Health, Iowa. pp 23-41.
- Tokuriki, M., Otsuki, R., Kai, M., Hiraga, A. and Aoki, O. (1997) Electromyographic activity of trunk muscles in horses during locomotion on a treadmill. In: *Proceedings of the 5th World Equine Veterinary Association Congress*, p 26.
- Townsend, H.G.G., Leach, D.H. and Fretz, P.B. (1983) Kinematics of the equine thoracolumbar spine. *Equine vet. J.* **15**, 117-122.
- Vasavada, A.N., Li, S. and Delp, S.L. (1998) Influence of muscle morphometry and moment arms on the moment-generating capacity of human neck muscles. *Spine* **23**, 412-422.
- Wakeling, J.M., Ritruethai, P., Dalton, S. and Nankervis, K. (2007) Segmental variation in the activity and function of the equine longissimus dorsi muscle during walk and trot. *Equine Comp. Exerc. Physiol.* **4**, 95-103.
- van Weeren, P.R. and Barneveld, A. (1986) A technique to quantify skin displacement in the walking horse. *J. Biomech.* **19**, 879-883.
- Whelan, P.J. (2003) Electromyogram recordings from freely moving animals. *Methods* **30**, 127-141.
- Winter, D.A., Fuglevand, A.J. and Archer, S.E. (1994) Crosstalk in surface electromyography: theoretical and practical estimates. *J. Electromyogr. Kinesiol.* **4**, 15-26.
- Zaneb, H., Kaufmann, V., Stanek, C., Peham, C. and Licka, T. (2009) Quantitative differences in activities of back and pelvic limb muscles during walking and trotting between chronically lame and nonlame horses. *Am. J. vet. Res.* **70**, 1129-1134.